



Published in final edited form as:

Brain Stimul. 2023 ; 16(5): 1401–1411. doi:10.1016/j.brs.2023.09.002.

Forniceal deep brain stimulation in a mouse model of Rett syndrome increases neurogenesis and hippocampal memory beyond the treatment period

Qi Wang^{a,b,1}, Bin Tang^{a,b,1}, Shuang Hao^{a,b,1,2}, Zhenyu Wu^{a,b}, Tingting Yang^{a,b,3}, Jianrong Tang^{a,b,*}

^aJan and Dan Duncan Neurological Research Institute, Texas Children's Hospital, Houston, TX 77030, USA

^bDepartment of Pediatrics, Baylor College of Medicine, Houston, TX 77030, USA

Abstract

Background: Rett syndrome (RTT), caused by mutations in the X-linked gene encoding methyl-CpG binding protein 2 (MeCP2), severely impairs learning and memory. We previously showed that forniceal deep brain stimulation (DBS) stimulates hippocampal neurogenesis with concomitant improvements in hippocampal-dependent learning and memory in a mouse model of RTT.

Objectives: To determine the duration of DBS benefits; characterize DBS effects on hippocampal neurogenesis; and determine whether DBS influences *MECP2* genotype and survival of newborn dentate granular cells (DGCs) in RTT mice.

Methods: Chronic DBS was delivered through an electrode implanted in the fimbria-fornix. We tested separate cohorts of mice in contextual and cued fear memory at different time points after DBS. We then examined neurogenesis, DGC apoptosis, and the expression of brain-derived neurotrophic factor (BDNF) and vascular endothelial growth factor (VEGF) after DBS by immunohistochemistry.

Results: After two weeks of forniceal DBS, memory improvements lasted between 6 and 9 weeks. Repeating DBS every 6 weeks was sufficient to maintain the improvement. Forniceal DBS stimulated the birth of more MeCP2-positive than MeCP2-negative DGCs and had no effect on DGC survival. It also increased the expression of BDNF but not VEGF in the RTT mouse dentate gyrus.

*Corresponding author: jtang1@bcm.edu.

¹These authors contributed equally.

²Present address: College of Life and Health Sciences, Northeastern University, Shenyang 110169, China

³Present address: Department of Neurology, Nanfang Hospital, Southern Medical University, Guangzhou 510515, China

Credit author statement

J.T. conceived and designed the study. Q.W., B.T., S.H., Z.W. and T.Y. performed the experiments and analyzed the data. Q.W., B.T., S.H. and J.T. wrote the manuscript with input from all co-authors.

Declaration of competing interest

None.

Conclusion: Improvements in learning and memory from forniceal DBS in RTT mice extends well beyond the treatment period and can be maintained by repeated DBS. Stimulation of BDNF expression correlates with improvements in hippocampal neurogenesis and memory benefits.

Keywords

deep brain stimulation; fornix; hippocampus; neurogenesis; fear memory; Rett syndrome

Introduction

Rett syndrome (RTT) is a devastating neurodevelopmental disorder that primarily affects females, as it is caused by mutations in the X-linked gene that encodes methyl CpG-binding protein 2 (MeCP2) [1, 2]. Girls with classic RTT appear to develop normally in their first year or two of postnatal life, but then undergo a period of behavioral regression during which they lose most of the motor, social, cognitive and language skills that they had developed, and develop autistic behaviors, breathing abnormalities, seizures, and a variety of other difficulties [3–5]. The delayed onset is due to the fact that the expression of MeCP2 protein greatly increases in mature neurons, where it binds methylated DNA to influence the expression of thousands of genes [2, 6]. With insufficient MeCP2, mature neurons appear to be unable to maintain synaptic plasticity [5]. Mouse models with MeCP2 loss of function, either through deletions or point mutations, recapitulate the major RTT symptoms including cognitive deficits. Deficits of hippocampus-dependent learning and memory and hippocampal synaptic plasticity are reproducibly observed across different RTT models [7–12]. Since the loss of cognitive skills is one of the most tragic aspects of RTT, there has been intense interest in finding therapeutic approaches that might mitigate this loss.

Deep brain stimulation (DBS) might provide such an approach. In recent years the use of DBS has expanded beyond its original applications in movement disorders to impairments in cognition and mood in adults [13–16] and, more recently, motor and neuropsychiatric disorders in children [17–19]. Inspired by a study showing that fornix/hypothalamus DBS can improve memory in Alzheimer’s disease (AD) [20], several years ago we tested forniceal DBS in a mouse model of RTT to see whether it could improve learning and memory in RTT mice (female *Mecp2*^{+/-}). We found that two weeks of DBS (1 h per day) in the right fimbria-fornix rescues hippocampal learning and memory in the contextual fear and Morris water maze tests, restores hippocampal synaptic plasticity, and increases adult hippocampal neurogenesis in RTT mice [11]. (We chose the right medial temporal lobe because it is more responsible for visuospatial learning and memory [21–23] and to avoid the risk of over-stimulating neurogenesis with bilateral implants, as high rates of neurogenesis correlate with forgetting [24].) These findings demonstrated the potential of DBS to mitigate learning and memory deficits in RTT.

At the time, we did not investigate how long these benefits might last. In the case of movement disorders, most notably Parkinson’s disease, DBS effects decay after stimulation is discontinued. If the memory benefits of forniceal DBS are due to neurogenesis, however, they might well last beyond the cessation of treatment. We therefore sought to determine the duration of benefits from two-week unilateral forniceal DBS, whether this improvement

could be prolonged by repeating DBS treatment, and if so, the optimal frequency for such treatments. We then evaluated DBS-induced hippocampal neurogenesis at different post-DBS time points corresponding to behavioral improvements at those stages. We also sought to understand how forniceal DBS exerts its benefits in RTT mice in the hope that better understanding of the functional effects of DBS will facilitate its translation into the clinic.

Material and Methods

Mice

We and others have demonstrated that female *Mecp2*^{+/-} mice [25] show impairments in contextual fear memory starting from the age of 8 weeks, after the mice enter the period of regression [9, 11, 26, 27]. We chose female mice again for the current study because of their clinical relevance. In addition, because we need to reliably target the fimbria-fornix for DBS throughout the experimental period, without the confound of large head size changes during development, we chose again to implant electrodes in mice that were 6 to 8 weeks old [11]. Female RTT mice (*Mecp2*^{+/-}) and wild-type (*Mecp2*^{+/+}, WT) littermates on an FVB.129 background were maintained on a 12 h light:12 h dark cycle (light on at 7:00 am) with standard mouse chow and water *ad libitum* in our onsite AAALAC-accredited facility. Prior to surgery, the mice were group-housed up to 5 mice per cage in a room maintained at 22°C. After surgery, the mice were singly housed.

All the experimental procedures and tests were conducted during the light cycle. The number of mice used per study group in each experiment are indicated in the relevant figure legends. All experimental and animal care procedures were approved by the Baylor College of Medicine Institutional Animal Care and Use Committee.

DBS surgery

DBS electrodes were implanted as previously described [11, 28, 29]. Briefly, 6-to 8-week-old mice were secured on a stereotaxic frame (David Kopf), anesthetized under 1-2% isoflurane, and implanted with a bipolar stimulation electrode constructed with Teflon-coated tungsten wire (bare diameter 50 µm, A-M system). Based on previous studies showing the right medial temporal lobe is more likely responsible for visuospatial learning and memory [21–23], the electrodes were targeted unilaterally to the right fimbria-fornix (0.2 mm posterior, 0.24 mm lateral, 2.3 mm ventral to the bregma) [29, 30] under the guidance of evoked potentials recorded in the ipsilateral dentate gyrus (DG; 1.8-2.0 mm posterior, 1.4-1.6 mm lateral, 2.2-2.3 mm ventral to the bregma), as previously described [11, 28]. All electrodes and attached connector sockets were fixed on the skull by dental cement. Animals were then individually housed with nesting material and given at least 1 week to recover after surgery.

After recovery, both RTT mice and WT littermates were randomly assigned to DBS or sham groups. Animals in the DBS groups received 1 h DBS daily for 14 consecutive days unless otherwise stated. The chronic DBS consisted of biphasic rectangular pulses (130 Hz, 60 µs pulse duration, negative first), while the stimulus intensities (30-50 µA) were individually

optimized to 80% of the threshold that elicited an after-discharge in the hippocampus. Sham groups underwent the same procedures but without stimulation delivery. Mice underwent behavioral tests or immunohistochemical examinations at specific intervals after DBS/sham treatment.

Additional cohort of mice at the age of 6 - 8 weeks were implanted with DBS electrodes targeting the right somatosensory cortex (0.4 mm anterior, 3.0 mm lateral, 2.3 mm ventral to the bregma) [30]. After recovery, these mice received DBS (biphasic rectangular pulses, negative first, 130 Hz, 60 μ s pulse duration, 50 μ A stimulus intensity) or sham treatment 1 h daily for 2 weeks, the same DBS/sham settings as in the fimbria-fornix [11, 28, 29] because this is a control experiment for the DBS target. Three weeks after the last day of the DBS/sham treatment, all the mice experienced the fear conditioning task.

Fear conditioning task

We used classic fear conditioning paradigm to evaluate hippocampus- and amygdala-dependent contextual fear memory as well as amygdala-dependent cued fear memory [31–33]. The fear conditioning task was performed as previously described [11, 28]. Briefly, a fear conditioning chamber is located within a sound-attenuating box, with a grid floor that could deliver electric shock. An overhead digital camera, a loudspeaker, and a house light were set up in the box. On the day of training, animals were placed in the conditioning chamber (cleaned with 70% ethanol) and left undisturbed for 2 min, after which a tone (30 s, 5 kHz, 80 dB) co-terminated with a scrambled foot shock (2 s, 0.7 mA). The tone/foot-shock stimuli were repeated after 1 min. The animals were returned to their home cage after staying in the chamber for an additional 1 min. Fear memory retention was evaluated 24 h after the training: mice were first recorded for 5 min in the same conditioning chamber (cleaned with 70% ethanol) without tone or foot shock for contextual fear memory and then tested in a novel cage (scented with 1% acetic acid) for a cued fear memory test in which the animals acclimated to the cage for 5 min and then heard a 5-min tone. The ANY-maze tracking system (Stoelting) was used to record the mice's behavior. Freezing, defined as an absence of any movement except for respiration [34], was scored only if the animal was immobile for at least 1 s [35]. The percentage of freezing time during the tests served as an index of fear memory. Cued fear memory was the difference between freezing time percentages in the tone phase versus the no-tone phase.

Open field

The open field apparatus consisted of a clear, open Plexiglas box (40×40×30 cm, Stoelting) fitted with an overhead camera and photo beams to record movements [11, 28]. Total distance traveled and average moving velocity were quantified over a 30-min period by ANY-maze (Stoelting).

Light/dark box

The light/dark box consisted of a clear Plexiglas chamber (40×20×30 cm) with an open top and a covered black chamber (40×20×30 cm), separated by a black partition with a small opening (Stoelting) [11, 28]. Mice were placed into the illuminated side and allowed to explore freely for 10 min; an entry was counted only when 50% of body length was in

either the light or dark compartment. The ANY-maze system with photo beam and overhead camera (Stoelting) was used to score the mice for the number of entries into the light compartment.

Elevated plus maze

The elevated plus maze was constructed from Plexiglas and consisted of two open arms (35×5 cm) and two closed arms ($35 \times 5 \times 15$ cm) extended from a central platform (5×5 cm) elevated 50 cm above the floor (Stoelting) [11, 28]. Mice were individually placed in the center square and allowed to freely explore the apparatus for 10 min. Activity was recorded with an overhead camera. Time spent in the open arm (counted only when 50% of body length was in an arm) was scored by ANY-maze.

Pain threshold

At the end of the test battery, mice were placed into the fear conditioning chamber [11]. Every 30 s, a 2-s scrambled electric foot shock with 0.05 mA increments (starting from 0 mA) was applied. The shock current thresholds of flinch, vocalization, and jumping were each recorded.

Histology

At the end of experiments, mice were euthanized with an overdose of isoflurane. An anodal current (25 μ A, 10 s) was passed through the electrode wire to verify the electrode placements. Frozen 30 μ m coronal sections were cut and stained with cresyl violet for histologic examination.

Immunohistochemistry

To evaluate neurogenesis in the DG over the two weeks of DBS/sham treatment or a comparable time frame, separate cohorts of mice were injected daily with 5-Bromo-2'-deoxyuridine (BrdU, Sigma-Aldrich, 75 mg/kg, i.p., once per day) for 12 days (days 3-14 of the 2-week DBS/sham session) to capture the ongoing birth of new neurons. Animals were perfused right after BrdU treatment or at designated timepoints [11, 36, 37]. To identify brain regions that were activated by forniceal DBS, we assessed the expression of the *c-Fos* gene in the brain 60 min after 2 h of DBS or sham treatment.

For perfusion, animals were deeply anesthetized with isoflurane and transcardially perfused with 50 ml 0.1 M phosphate-buffered saline (PBS, PH 7.4) followed by 60 ml 4% paraformaldehyde (PFA) in 0.1 M PBS at 4°C. We harvested brains, post-fixed them in 4% PFA for 12 h, and then preserved them in 30% sucrose at 4°C for 2 days. We prepared floating coronal sections (50 μ m thickness) by cryostat (Leica) and performed immunohistochemistry for *c-Fos*, Doublecortin (DCX), BrdU, MeCP2, Caspase-3, NeuN, brain-derived neurotrophic factor (BDNF), or vascular endothelial growth factor (VEGF), respectively, after incubation in blocking solution (0.3% Triton X-100, 5% normal goat serum in 0.1 M PBS) for 1 h at room temperature (RT) followed by 48 h incubation with primary antibody at 4°C.

Primary antibodies and their final concentrations were as follows: rabbit polyclonal anti-*c-Fos* (1: 250, MA5-15055, Invitrogen, USA), rabbit anti-DCX (1:400, #4604, Cell Signaling Technology, USA), rat monoclonal anti-Bromodeoxyuridine (BrdU) (1:140, OBT0030, Accurate Chemical & Scientific Corporation, USA), rabbit anti-MeCP2 (1:800, #3456, Cell Signaling Technology, USA), rabbit anti-Caspase-3 (1:250, #9664, Cell Signaling Technology, USA), mouse anti-NeuN (1:200, MAB377, Millipore, USA), rabbit polyclonal anti-BDNF (1:800, AB1534, Millipore, USA), mouse anti-VEGF (1:20, Sc-7269, Santa Cruz Biotechnology, USA). Sections were incubated with corresponding secondary antibodies for 2 h before counterstaining with 4', 6-diamidino-2-phenylindole (DAPI) (900 nM, D1036, Invitrogen, USA) for 15 min at RT in darkness. Secondary antibodies and their final concentrations were as follows: Alexa fluor 568 goat anti-rabbit IgG (1:500, A11036, Invitrogen, USA), Alexa fluor 488 goat anti-rat IgG (1:500, A11006, Invitrogen, USA), Alexa fluor 633 goat anti-mouse IgG (1:500, A21050, Invitrogen, USA). The sections were washed three times with 0.1 M PBS and mounted on glass using Fluoromount-G (Southern Biotech, USA). For *c-Fos* staining, sections were pretreated with 0.3% H₂O₂ in PBS for 30 min at RT. For BrdU detection, sections were pretreated with 2 M HCl for 30 min at 37°C and washed in 0.1M borate buffer (pH 8.4) for 10 min.

Imaging and quantification

Z stacks of 2 µm thick single-plane images were obtained with a laser scanning microscope (LSM 710, Carl Zeiss) at 20x magnification. Settings for obtaining the images (e.g., pinhole size, gain, and offset) were kept constant throughout all the experiments. Each slice had 12-13 z-axis optical slices. Digital images were routed to a Windows PC for quantitative analyses using ImageJ software (NIH). DCX-, BrdU-, MeCP2-, Caspase-3-, NeuN-, *c-Fos*-, BDNF-, and VEGF-positive cells were assessed through the entire z-axis of each slice. For quantification, six sections per mouse brain were counted. Resulting cell numbers were multiplied by 6 to obtain the estimated total number of positive cells per DG [11, 38, 39].

Statistical analysis

GraphPad Prism (version 8.3.0, GraphPad Software, San Diego, CA) was used for all statistical analyses and to create all plots. We used the Shapiro-Wilk test to ascertain normal distribution and the two-tailed unpaired *t*-test or Mann-Whitney test (if data were not normally distributed) for two-sample comparisons. We used two-way analysis of variance (ANOVA) followed by Tukey *post hoc* analysis for multiple-group comparisons unless otherwise stated.

Results

Forniceal DBS-induced memory improvement wanes after 6 weeks

The classic fear conditioning task is widely used to evaluate contextual and cued fear memory. During fear conditioning, animals form an association between a neutral conditioned stimulus (e.g., a tone) and an aversive unconditioned stimulus (e.g., an electric foot shock). As a result, subsequent exposure to the conditioned stimulus will evoke a variety of behavioral, endocrine, and autonomic responses that are typically elicited in dangerous situations [31, 32]. To determine the duration of DBS-induced memory

enhancement, we tested contextual and cued fear memory at 6 and 9 weeks after the 2-week DBS or sham treatment (Fig. 1A–D). At six weeks, DBS-treated RTT mice showed more contextual freezing than the sham-treated RTT group ($p = 0.046$). Indeed, there was no significant difference between the RTT-DBS and the WT-sham groups ($p = 0.548$). DBS did not alter contextual fear memory in WT littermates ($p = 0.856$) or cued fear memory in either RTT mice ($p = 0.199$) or WT controls ($p = 0.720$) (Fig. 1E–G; Supplementary Table 1 contains statistics for every experiment). We then tested fear memory at 9 weeks post-treatment in a separate cohort of RTT mice. By this point, there were no significant differences between DBS- and sham-treated groups in contextual fear memory ($p = 0.504$) or in cued memory ($p = 0.751$) (Fig. 1H–J).

To ensure that there were no differences between RTT and WT mice in locomotor activity that would confound the detection of freezing behavior. We tested the mice in the open field assay and found no difference in motor activity between RTT mice and their WT littermates (Supplementary Fig. 1A–C). All groups of mice traveled similar distance in the first 5 min, matching the time window for the fear memory test [28]. The hippocampal memory benefit induced by two-week fornical DBS in RTT mice thus lasts for at least 6 weeks but not as long as 9 weeks.

Repeated fornical DBS maintains memory improvements

Because the benefits of 2 weeks of daily DBS waned after 6 weeks, we delivered three runs of the same 2-week fornical DBS or sham treatment at 6-week intervals and evaluated fear memory three weeks after the last run of DBS/sham treatment, when the mice were 30 weeks old (Fig. 2A). The three courses of DBS treatment did not change the body weight or pain threshold in either genotype (Supplementary Fig. 1D and E). RTT-sham mice had impaired contextual fear memory compared to WT-sham controls ($p = 0.003$). Repeated DBS treatment increased contextual freezing in RTT mice ($p = 0.004$) and rescued their memory to the level of WT littermates ($p = 0.936$). Cued fear memory was not altered in either RTT mice ($p = 0.806$) or WT controls ($p = 0.774$) after DBS treatment (Fig. 2B–D).

To test whether the observed memory benefit is specific to the brain region target of DBS, we needed to identify brain regions not activated by fornical DBS to serve as a negative control [11]. We therefore assessed the expression of immediate early gene *c-Fos* after 2-h fornical DBS/sham treatment. There was no change of *c-Fos* expression in the somatosensory cortex after fornical DBS in either RTT mice ($p = 0.742$) or WT littermates ($p = 0.214$) (Supplementary Fig. 2A, B), so we implanted DBS electrodes there in RTT mice and WT littermates and treated them with 2-week DBS or sham treatment, as we did in the fimbria-fornix. Three weeks later, all the animals underwent the fear conditioning task (Supplementary Fig. 2C). DBS of the somatosensory cortex did not alter contextual fear memory in either RTT mice ($p = 0.373$) or WT littermates ($p = 0.896$) (Supplementary Fig. 2D). It also did not alter the levels of anxiety or locomotion in RTT mice or WT littermates (Supplementary Fig. 2E–H). DBS-induced learning and memory benefits in RTT mice are therefore target-specific.

Forniceal DBS-induced neurogenesis corresponds with contextual learning improvement

Adult hippocampal neurogenesis contributes to hippocampal long-term synaptic plasticity and hippocampus-dependent learning and memory [40–42]. We previously showed that forniceal DBS increases hippocampal neurogenesis in the DG when tested right after DBS, which corresponds with improved contextual fear memory 3 weeks later [11]. We now sought to determine whether this correspondence holds at later time points following DBS.

Since it takes 2-5 weeks for newborn DGCs to mature and functionally integrate into the neural network [43–46], DGCs born in 12- to 14-week-old mice engage in hippocampal function at ~17 weeks of age, matching the age at which we tested memory 6 weeks after treatment (Fig. 1A). To label newborn cells we injected BrdU each day for 12 days before perfusion (Fig. 3A) [11]. We then measured the number of cells that were positive for BrdU, DCX (Doublecortin, to label the immature neurons), or both (Fig. 3B). Baseline levels of dentate neurogenesis in RTT-sham mice were significantly lower than in WT-sham littermates (BrdU⁺, $p = 0.006$; DCX⁺, $p = 0.019$; BrdU⁺/DCX⁺, $p = 0.028$) (Fig. 3C–E), but forniceal DBS rescued these numbers in RTT mice (BrdU⁺, $p < 0.001$; DCX⁺, $p < 0.001$; BrdU⁺/DCX⁺, $p < 0.001$) to levels roughly equivalent to those of the WT-sham group (BrdU⁺, $p = 0.090$; DCX⁺, $p = 0.394$). In fact, the number of BrdU⁺/DCX⁺ cells in RTT-DBS mice was even higher than that in WT-sham mice ($p = 0.018$). DBS also increased the BrdU⁺/DCX⁺ cells in WT mice ($p = 0.05$).

We measured neurogenesis that occurred between 15 and 17 weeks of age in RTT mice, matching the memory testing 9 weeks after DBS/sham treatment (Fig. 1A, Fig. 3A, F). Forniceal DBS did not change the number of BrdU⁺ ($p = 0.258$) or BrdU⁺/DCX⁺ cells ($p = 0.113$) but tended to increase the total number of DCX⁺ cells ($p = 0.0526$) (Fig. 3G–I).

Forniceal DBS preferentially induces the birth of more MeCP2-positive neurons

MeCP2 expression in heterozygous females is mosaic due to random X chromosome inactivation, so newborn neurons in RTT mice can be either MeCP2⁺ or MeCP2⁻. To understand how DBS affects neurogenesis, we counted the MeCP2-expressing cells labeled by BrdU during DBS treatment. BrdU was injected immediately after daily DBS/sham treatment for 12 days and the mice were perfused three weeks later to allow MeCP2 expression in mature BrdU-labeled DGCs (Fig. 4A). The brain sections containing the DG were immunostained with antibodies against MeCP2, NeuN (labeling mature neurons), and BrdU (Fig. 4B). At baseline, RTT-sham mice had lower levels of newborn DGCs (BrdU⁺, $p = 0.032$; BrdU⁺/NeuN⁺ double staining, $p = 0.022$, and BrdU⁺/NeuN⁺/MeCP2⁺ triple staining, $p = 0.006$) (Fig. 4C–E). Forniceal DBS increased the numbers of these cell types in both RTT mice (BrdU⁺, $p < 0.001$; BrdU⁺/NeuN⁺, $p < 0.001$; BrdU⁺/NeuN⁺/MeCP2⁺, $p < 0.001$) and WT littermates (BrdU⁺, $p = 0.002$; BrdU⁺/NeuN⁺, $p = 0.002$; BrdU⁺/NeuN⁺/MeCP2⁺, $p = 0.002$) compared to their respective sham-treated controls. Consistent with our previous report [11], forniceal DBS stimulated neurogenesis so well that DBS-treated RTT mice had even higher numbers of BrdU⁺ ($p = 0.010$), BrdU⁺/NeuN⁺ ($p < 0.001$), and BrdU⁺/NeuN⁺/MeCP2⁺ DGCs ($p = 0.020$) cells than sham-treated WT animals. As a result, the ratio of BrdU⁺/NeuN⁺/MeCP2⁺ cells over total BrdU⁺/NeuN⁺ cells in RTT-DBS mice was significantly higher than that in the RTT-sham group ($p < 0.001$, Fig. 4F).

Since neuronal birth and death are coordinated to establish and maintain properly functioning neural circuits [47, 48], we wondered whether forniceal DBS influences cell survival. Given that MeCP2 participates in suppressing the apoptosis of DGCs by repressing caspase-3 signaling [49–51], we detected apoptosis by staining caspase-3 following the same experimental setting (Fig. 4A). There was no difference among the four groups ($p = 0.337$; Fig. 4G, H). Thus, neither MeCP2 loss nor forniceal DBS alters apoptosis in the DG of RTT mice or WT littermates, at least at 3 weeks after the DBS/sham treatment. Forniceal DBS therefore acts by inducing the birth of more MeCP2⁺ than MeCP2⁻DGCs, or, put slightly differently, MeCP2⁺ neurons are better able to respond to DBS.

Forniceal DBS stimulates the expression of BDNF but not VEGF

Neurotrophic factors such as BDNF and VEGF play essential roles in hippocampal neurogenesis, long-term synaptic plasticity, and memory [52–57]. It has been shown that DBS influences the expression of these neurotrophic factors in the hippocampus [58] and other brain regions [59, 60]. Moreover, loss of MeCP2 function has been shown to alter the expression of BDNF and VEGF [61, 62]. To determine whether forniceal DBS modulates BDNF and/or VEGF expression in the DG in RTT mice [11, 28], we examined the expression of both neurotrophins in the DG using immunohistochemistry after 2-week DBS treatment (Fig. 5A–C).

The sham-treated RTT mice showed lower BDNF expression than sham-treated WT littermates ($p = 0.015$). Forniceal DBS increased BDNF expression in RTT mice ($p = 0.017$) to the level of sham-treated WT littermates ($p = 0.964$) (Fig. 5B) but did not increase BDNF expression in WT littermates ($p = 0.720$).

MeCP2 loss did not alter VEGF expression in RTT-sham mice compared to WT-sham controls ($p = 0.622$). In fact, forniceal DBS actually suppressed VEGF expression in both RTT mice ($p < 0.001$) and WT controls ($p < 0.001$) (Fig. 5C). These results suggest that chronic forniceal DBS differentially regulates the expression of neurotrophic factors in the dentate gyrus.

Discussion

The benefits of forniceal DBS on learning and memory have been studied in patients and animal models of AD [16, 20, 63], mouse models of intellectual disability disorders [11, 28], and experimental models of dementia in rats [64, 65] under various conditions (e.g., different target sites, electric pulse parameters, acute or chronic treatment duration, with or without anesthesia, etc.). The mechanisms underlying forniceal DBS-induced memory benefits are likely multifold [66, 67]. First, forniceal DBS may act both locally and remotely through myelinated axons (orthodromic and antidromic) to restore specific neural network activity related to the diseases [68–71]: it increases neuronal activity in the hippocampus and other limbic system structures [11, 72, 73], and chronic forniceal DBS restores feedforward inhibition in the dentate gyrus in a mouse model of CDKL5 deficiency disorder (CDD) [28]. Second, forniceal DBS promotes the release of neurotransmitters that are important for memory function. For instance, acute forniceal DBS enhanced acetylcholine (but not glutamate) level in the hippocampus [72] and dopamine release in the nucleus accumbens

[73]. Acute DBS of the fornix also increased the expression of neurotrophins (e.g., BDNF and VEGF) that are crucial for hippocampal neurogenesis, long-term potentiation (LTP) of synaptic transmission, and memory function [58]. Third, forniceal DBS may enhance hippocampal synaptic plasticity. Recent studies demonstrated that chronic forniceal DBS enhanced LTP in the perforant path to the dentate gyrus pathway in freely moving WT and/or transgenic mice modeling RTT and CDD [11, 28]. Fourth, chronic forniceal DBS globally increased the brain glucose metabolism in AD patients [16, 74, 75]. Acute DBS of the fornix also increases glucose consumption in the hippocampus of aged mice [76]. Finally, and consistent with the current report, several studies have shown that DBS of the brain structures or pathways connecting the hippocampus induces hippocampal neurogenesis [11, 38, 65, 77–79]. This effect is paralleled by improved hippocampal LTP and hippocampal-dependent contextual or spatial learning and memory [11, 77], although another study did not see an association between memory enhancement and neurogenesis after acute DBS of the fornix under different experimental settings [65]. Experimental conditions thus seem to be quite important. This may be the case with studying neurogenesis in general. Despite some controversy [80, 81], a large body of evidence supports the existence of human adult hippocampal neurogenesis under both normal and disease conditions [82, 83] in humans and experimental animal models [84, 85].

The necessity of continuous DBS to treat motor symptoms [86, 87] led to the proposal that DBS benefits result from “depolarization blockade,” i.e., the suppression of neuronal activity in the DBS sites [88–90]. The benefits of DBS on learning and memory, however, persist after DBS termination, so depolarization blockade does not seem to apply to cognitive benefits. Besides the evidence presented here, previous studies in mouse models of AD have shown that acute DBS in the fornix or entorhinal cortex improves hippocampal memory 4–6 weeks after DBS [63, 91]. Some Alzheimer’s patients receiving sustained forniceal DBS over 12 months showed better hippocampus-dependent spatial memory 6 or 12 months after DBS was begun [16, 20]. These pre-clinical data are particularly important given that continuous stimulation drains the device’s battery much more quickly as compared to intermittent DBS administration. Moreover, it is worth pointing out that the duration and intensity of the DBS pulses in the current study were half or less than half of those used in other rodent studies [64, 65, 92].

In the present study, the most likely mechanism underlying memory improvement is adult hippocampal neurogenesis [77]. Both memory and corresponding neurogenesis were enhanced when memory was tested 3 and 6 weeks after DBS, respectively [11], but disappeared 9 weeks after treatment. Moreover, a previous study demonstrated that pharmacological suppression of dentate neurogenesis blocks spatial memory enhancement caused by DBS of the entorhinal cortex, lending further support to the notion that adult neurogenesis underlies DBS-induced hippocampal memory benefits [77]. It is not yet possible to speculate intelligently on how one would translate the current study in RTT mice into human terms, except to note that the duration of treatment effects in mice roughly parallels the length of time it takes for the neurons born during DBS treatment to find their way and integrate into the circuit (and that human newborn neurons take longer to mature [93]).

Interestingly, DBS altered the genotypic composition of the hippocampal circuit in the female RTT mice: MeCP2-positive cells constitute roughly 50% of the neural circuit before DBS but up to ~80% of newborn cells afterward. It may be that only MeCP2-positive cells are healthy enough to be able to respond to DBS by releasing BDNF, which plays a crucial role in hippocampal neurogenesis, synaptic plasticity, and memory [94–96].

In fact, growing evidence supports the role of neurotrophic factors in mediating the effects of DBS. Although different experimental protocols and different models indicate that DBS can have divergent effects on different neurotrophins, the upregulation of BDNF is a consistent finding. In the current study, we observed increased BDNF expression in RTT mice but diminished VEGF expression in both RTT mice and their WT controls after chronic DBS (1 h daily for two weeks). A previous DBS study in rats found that acute stimulation of the fornix (1 h under anesthesia) increased the expression of BDNF and VEGF, but not glial cell-derived neurotrophic factor (GDNF) [58]. Another study showed that chronic DBS in the subthalamic nucleus (24 h/day for two weeks) in a rat model of Parkinson's disease upregulated BDNF, VEGF, and GDNF protein levels in the ipsilateral striatum but in the motor cortex increased only BDNF [97]. BDNF upregulation thus seems crucial in mediating the benefits of DBS, in multiple brain regions and disease contexts. In the case of Rett syndrome, it has been appreciated for some time that MeCP2 loss-of-function mutant mice have low BDNF levels and impaired axonal transport [98]. Overexpression of BDNF in the RTT mouse brain has not been very successful, but restoring BDNF transport in the cortico-striatal circuit in *Mecp2* mutant mice rescues motor incoordination, body weight, and breathing dysrhythmias [99]. The fact that DBS enhanced BDNF levels in our RTT mice but did not affect body weight or hyperactivity, two features associated with low BDNF in RTT mice [100], indicates that the effects of fornical DBS remained very local. Thus, although the electrical field generated by DBS can activate neural tissue adjacent to the stimulus site, this seems not to have occurred in the present study. We believe there are two reasons for this. First, we delivered bipolar pulses, which require lower intensities than monopolar [101], and we then optimized the pulse intensities to below the threshold that evokes an afterdischarge in the hippocampus [11, 21, 28, 102]. Second, both the duration and intensity of the DBS pulses in this study were much less than those commonly used in other rodent studies [64, 65, 92].

One limitation of the current study is that we examined BDNF and VEGF expression only at one timepoint (immediately after the DBS/sham session) and under a specific DBS setting (e.g., 2-week chronic DBS). Further experiments with different settings would allow more exploration of fornical DBS-induced modulation of neurotrophin expression. Another limitation is that we did not evaluate the effectiveness of bilateral fornical DBS, though as noted in the introduction, too much neurogenesis is associated with forgetting [24], and unilateral DBS already stimulated more neurogenesis in the RTT mice than in sham-treated WT mice. Lastly, there might be difference between the effect induced by DBS in white matter (e.g., the fimbria-fornix) and gray matter (e.g., the somatosensory cortex) [22, 103]. In other words, another white matter target could serve as a control site for fornical DBS in future studies. Nevertheless, our sham groups in both genotypes should serve as proper controls.

In conclusion, two weeks of fornical DBS rescues hippocampal learning and memory for at least six weeks after termination of treatment, and the benefit can be maintained by repeating treatment every six weeks. The potential of DBS to stimulate neurogenesis has implications for many more common disorders that involve suppression or loss of neurogenesis, such as depression [104, 105].

Supplementary Material

Refer to Web version on PubMed Central for supplementary material.

Acknowledgements

This research was supported by the National Institute of Neurological Disorders and Stroke (R01NS100738 and 2R01NS100738 to J.T.), the Eunice Kennedy Shriver National Institute of Child Health and Human Development (U54HD083092, P50HD103555 to Baylor College of Medicine Intellectual and Developmental Disabilities Research Center, Neuroconnectivity Core, Neurovisualization Core), the *In Vivo* Neurophysiology Core of the Jan and Dan Duncan Neurological Research Institute at Texas Children's Hospital, the Chao Family Foundation, and the Cockrell Family Foundation. We thank V. Brandt and B.E. Siegel for critical reading of this manuscript.

References

- [1]. Ip JPK, Mellios N, Sur M. Rett syndrome: insights into genetic, molecular and circuit mechanisms. *Nat Rev Neurosci* 2018;19(6):368–82. 10.1038/s41583-018-0006-3. [PubMed: 29740174]
- [2]. Chahrour M, Zoghbi HY. The story of Rett syndrome: from clinic to neurobiology. *Neuron* 2007;56(3):422–37. 10.1016/j.neuron.2007.10.001. [PubMed: 17988628]
- [3]. Hagberg B, Aicardi J, Dias K, Ramos O. A progressive syndrome of autism, dementia, ataxia, and loss of purposeful hand use in girls: Rett's syndrome: report of 35 cases. *Ann Neurol* 1983;14(4):471–9. 10.1002/ana.410140412. [PubMed: 6638958]
- [4]. Neul JL, Kaufmann WE, Glaze DG, Christodoulou J, Clarke AJ, Bahi-Buisson N, et al. . Rett syndrome: revised diagnostic criteria and nomenclature. *Ann Neurol* 2010;68(6):944–50. 10.1002/ana.22124. [PubMed: 21154482]
- [5]. Sandweiss AJ, Brandt VL, Zoghbi HY. Advances in understanding of Rett syndrome and MECP2 duplication syndrome: prospects for future therapies. *Lancet Neurol* 2020;19(8):689–98. 10.1016/S1474-4422(20)30217-9. [PubMed: 32702338]
- [6]. Lewis JD, Meehan RR, Henzel WJ, Maurer-Fogy I, Jeppesen P, Klein F, et al. Purification, sequence, and cellular localization of a novel chromosomal protein that binds to methylated DNA. *Cell* 1992;69(6):905–14. 10.1016/0092-8674(92)90610-o. [PubMed: 1606614]
- [7]. Chao HT, Chen H, Samaco RC, Xue M, Chahrour M, Yoo J, et al. . Dysfunction in GABA signalling mediates autism-like stereotypies and Rett syndrome phenotypes. *Nature* 2010;468(7321):263–9. 10.1038/nature09582. [PubMed: 21068835]
- [8]. Moretti P, Levenson JM, Battaglia F, Atkinson R, Teague R, Antalffy B, et al. Learning and memory and synaptic plasticity are impaired in a mouse model of Rett syndrome. *J Neurosci* 2006;26(1):319–27. 10.1523/JNEUROSCI.2623-05.2006. [PubMed: 16399702]
- [9]. Samaco RC, McGraw CM, Ward CS, Sun Y, Neul JL, Zoghbi HY. Female *Mecp2*(+/-) mice display robust behavioral deficits on two different genetic backgrounds providing a framework for pre-clinical studies. *Hum Mol Genet* 2013;22(1):96–109. 10.1093/hmg/dds406. [PubMed: 23026749]
- [10]. Li H, Zhong X, Chau KF, Williams EC, Chang Q. Loss of activity-induced phosphorylation of MeCP2 enhances synaptogenesis, LTP and spatial memory. *Nat Neurosci* 2011;14(8):1001–8. 10.1038/nn.2866. [PubMed: 21765426]
- [11]. Hao S, Tang B, Wu Z, Ure K, Sun Y, Tao H, et al. . Fornical deep brain stimulation rescues hippocampal memory in Rett syndrome mice. *Nature* 2015;526(7573):430–4. 10.1038/nature15694. [PubMed: 26469053]

- [12]. Adachi M, Autry AE, Covington HE 3rd, Monteggia LM. MeCP2-mediated transcription repression in the basolateral amygdala may underlie heightened anxiety in a mouse model of Rett syndrome. *J Neurosci* 2009;29(13):4218–27. 10.1523/JNEUROSCI.4225-08.2009. [PubMed: 19339616]
- [13]. Lozano AM, Lipsman N, Bergman H, Brown P, Chabardes S, Chang JW, et al. . Deep brain stimulation: current challenges and future directions. *Nat Rev Neurol* 2019;15(3):148–60. 10.1038/s41582-018-0128-2. [PubMed: 30683913]
- [14]. Perlmutter JS, Mink JW. Deep brain stimulation. *Annu Rev Neurosci* 2006;29:229–57. 10.1146/annurev.neuro.29.051605.112824. [PubMed: 16776585]
- [15]. Aum DJ, Tierney TS. Deep brain stimulation: foundations and future trends. *Front Biosci (Landmark Ed)* 2018;23:162–82. 10.2741/4586.
- [16]. Lozano AM, Fosdick L, Chakravarty MM, Leoutsakos JM, Munro C, Oh E, et al. . A Phase II Study of Fornix Deep Brain Stimulation in Mild Alzheimer’s Disease. *J Alzheimers Dis* 2016;54(2):777–87. 10.3233/JAD-160017. [PubMed: 27567810]
- [17]. Servello D, Porta M, Sassi M, Brambilla A, Robertson MM. Deep brain stimulation in 18 patients with severe Gilles de la Tourette syndrome refractory to treatment: the surgery and stimulation. *J Neurol Neurosurg Psychiatry* 2008;79(2):136–42. 10.1136/jnnp.2006.104067. [PubMed: 17846115]
- [18]. Vidailhet M, Yelnik J, Lagrange C, Fraix V, Grabli D, Thobois S, et al. Bilateral pallidal deep brain stimulation for the treatment of patients with dystonia-choreoathetosis cerebral palsy: a prospective pilot study. *Lancet Neurol* 2009;8(8):709–17. 10.1016/S1474-4422(09)70151-6. [PubMed: 19576854]
- [19]. Borggraefe I, Mehrkens JH, Telegravciska M, Berweck S, Botzel K, Heinen F. Bilateral pallidal stimulation in children and adolescents with primary generalized dystonia—report of six patients and literature-based analysis of predictive outcomes variables. *Brain Dev* 2010;32(3):223–8. 10.1016/j.braindev.2009.03.010. [PubMed: 19403250]
- [20]. Laxton AW, Tang-Wai DF, McAndrews MP, Zumsteg D, Wennberg R, Keren R, et al. . A phase I trial of deep brain stimulation of memory circuits in Alzheimer’s disease. *Ann Neurol* 2010;68(4):521–34. 10.1002/ana.22089. [PubMed: 20687206]
- [21]. Suthana N, Haneef Z, Stern J, Mukamel R, Behnke E, Knowlton B, et al. . Memory enhancement and deep-brain stimulation of the entorhinal area. *N Engl J Med* 2012;366(6):502–10. 10.1056/NEJMoa1107212. [PubMed: 22316444]
- [22]. Mankin EA, Aghajan ZM, Schuette P, Tran ME, Tchemodanov N, Titiz A, et al. . Stimulation of the right entorhinal white matter enhances visual memory encoding in humans. *Brain Stimul* 2021;14(1):131–40. 10.1016/j.brs.2020.11.015. [PubMed: 33279717]
- [23]. Smith ML, Milner B. Right hippocampal impairment in the recall of spatial location: encoding deficit or rapid forgetting? *Neuropsychologia* 1989;27(1):71–81. 10.1016/0028-3932(89)90091-2. [PubMed: 2496329]
- [24]. Akers KG, Martinez-Canabal A, Restivo L, Yiu AP, De Cristofaro A, Hsiang HL, et al. . Hippocampal neurogenesis regulates forgetting during adulthood and infancy. *Science* 2014;344(6184):598–602. 10.1126/science.1248903. [PubMed: 24812394]
- [25]. Guy J, Hendrich B, Holmes M, Martin JE, Bird A. A mouse *Mecp2*-null mutation causes neurological symptoms that mimic Rett syndrome. *Nat Genet* 2001;27(3):322–6. 10.1038/85899. [PubMed: 11242117]
- [26]. Smith M, Arthur B, Cikowski J, Holt C, Gonzalez S, Fisher NM, et al. . Clinical and Preclinical Evidence for M(1) Muscarinic Acetylcholine Receptor Potentiation as a Therapeutic Approach for Rett Syndrome. *Neurotherapeutics* 2022;19(4):1340–52. 10.1007/s13311-022-01254-3. [PubMed: 35670902]
- [27]. Urbinati C, Cosentino L, Germinario EAP, Valenti D, Vigli D, Ricceri L, et al. . Treatment with the Bacterial Toxin CNF1 Selectively Rescues Cognitive and Brain Mitochondrial Deficits in a Female Mouse Model of Rett Syndrome Carrying a MeCP2-Null Mutation. *Int J Mol Sci* 2021;22(13). 10.3390/ijms22136739.

- [28]. Hao S, Wang Q, Tang B, Wu Z, Yang T, Tang J. CDKL5 deficiency augments inhibitory input into the dentate gyrus that can be reversed by deep brain stimulation. *J Neurosci* 2021. 10.1523/JNEUROSCI.1010-21.2021.
- [29]. Wang Q, Tang B, Tang J. Protocol for deep brain stimulation in the fimbria-fornix of freely moving mice. *STAR Protoc* 2022;3(1):101054. 10.1016/j.xpro.2021.101054. [PubMed: 35005636]
- [30]. Paxinos G, Franklin KBJ. *The Mouse Brain in Stereotaxic Coordinates*. San Diego, CA: Academic Press; 2001.
- [31]. LeDoux JE. Emotion circuits in the brain. *Annu Rev Neurosci* 2000;23:155–84. 10.1146/annurev.neuro.23.1.155. [PubMed: 10845062]
- [32]. Maren S. Neurobiology of Pavlovian fear conditioning. *Annu Rev Neurosci* 2001;24:897–931. 10.1146/annurev.neuro.24.1.897. [PubMed: 11520922]
- [33]. Phillips RG, LeDoux JE. Differential contribution of amygdala and hippocampus to cued and contextual fear conditioning. *Behav Neurosci* 1992;106(2):274–85. 10.1037/0735-7044.106.2.274. [PubMed: 1590953]
- [34]. Maren S, De Oca B, Fanselow MS. Sex differences in hippocampal long-term potentiation (LTP) and Pavlovian fear conditioning in rats: positive correlation between LTP and contextual learning. *Brain Res* 1994;661(1-2):25–34. 10.1016/0006-8993(94)91176-2. [PubMed: 7834376]
- [35]. Corcoran KA, Maren S. Hippocampal inactivation disrupts contextual retrieval of fear memory after extinction. *J Neurosci* 2001;21(5):1720–6. 10.1523/JNEUROSCI.21-05-01720.2001. [PubMed: 11222661]
- [36]. Kempermann G, Gast D, Kronenberg G, Yamaguchi M, Gage FH. Early determination and long-term persistence of adult-generated new neurons in the hippocampus of mice. *Development* 2003;130(2):391–9. 10.1242/dev.00203. [PubMed: 12466205]
- [37]. Gao Z, Ure K, Ding P, Nashaat M, Yuan L, Ma J, et al. . The master negative regulator REST/NRSF controls adult neurogenesis by restraining the neurogenic program in quiescent stem cells. *J Neurosci* 2011;31(26):9772–86. 10.1523/JNEUROSCI.1604-11.2011. [PubMed: 21715642]
- [38]. Encinas JM, Hamani C, Lozano AM, Enikolopov G. Neurogenic hippocampal targets of deep brain stimulation. *J Comp Neurol* 2011;519(1):6–20. 10.1002/cne.22503. [PubMed: 21120924]
- [39]. Song S, Song S, Cao C, Lin X, Li K, Sava V, et al. . Hippocampal neurogenesis and the brain repair response to brief stereotaxic insertion of a microneedle. *Stem Cells Int* 2013;2013:205878. 10.1155/2013/205878. [PubMed: 23554817]
- [40]. van Praag H, Kempermann G, Gage FH. Running increases cell proliferation and neurogenesis in the adult mouse dentate gyrus. *Nat Neurosci* 1999;2(3):266–70. 10.1038/6368. [PubMed: 10195220]
- [41]. Shors TJ, Miesegaes G, Beylin A, Zhao M, Rydel T, Gould E. Neurogenesis in the adult is involved in the formation of trace memories. *Nature* 2001;410(6826):372–6. 10.1038/35066584. [PubMed: 11268214]
- [42]. Stuchlik A. Dynamic learning and memory, synaptic plasticity and neurogenesis: an update. *Front Behav Neurosci* 2014;8:106. 10.3389/fnbeh.2014.00106. [PubMed: 24744707]
- [43]. Piatti VC, Davies-Sala MG, Esposito MS, Mongiat LA, Trincherro MF, Schinder AF. The timing for neuronal maturation in the adult hippocampus is modulated by local network activity. *J Neurosci* 2011;31(21):7715–28. 10.1523/JNEUROSCI.1380-11.2011. [PubMed: 21613484]
- [44]. Zhao C, Deng W, Gage FH. Mechanisms and functional implications of adult neurogenesis. *Cell* 2008;132(4):645–60. 10.1016/j.cell.2008.01.033. [PubMed: 18295581]
- [45]. Zhao C, Teng EM, Summers RG Jr, Ming GL, Gage FH. Distinct morphological stages of dentate granule neuron maturation in the adult mouse hippocampus. *J Neurosci* 2006;26(1):3–11. 10.1523/JNEUROSCI.3648-05.2006. [PubMed: 16399667]
- [46]. Ge S, Goh EL, Sailor KA, Kitabatake Y, Ming GL, Song H. GABA regulates synaptic integration of newly generated neurons in the adult brain. *Nature* 2006;439(7076):589–93. 10.1038/nature04404. [PubMed: 16341203]
- [47]. Gohlke JM, Griffith WC, Faustman EM. The role of cell death during neocortical neurogenesis and synaptogenesis: implications from a computational model for the rat and mouse. *Brain Res Dev Brain Res* 2004;151(1-2):43–54. 10.1016/j.devbrainres.2004.03.020. [PubMed: 15246691]

- [48]. Larson TA, Thatra NM, Lee BH, Brenowitz EA. Reactive neurogenesis in response to naturally occurring apoptosis in an adult brain. *J Neurosci* 2014;34(39):13066–76. 10.1523/JNEUROSCI.3316-13.2014. [PubMed: 25253853]
- [49]. Zhao LY, Tong DD, Xue M, Ma HL, Liu SY, Yang J, et al. . MeCP2, a target of miR-638, facilitates gastric cancer cell proliferation through activation of the MEK1/2-ERK1/2 signaling pathway by upregulating GIT1. *Oncogenesis* 2017;6(7):e368. 10.1038/oncsis.2017.60. [PubMed: 28759023]
- [50]. Zhao L, Liu Y, Tong D, Qin Y, Yang J, Xue M, et al. . MeCP2 Promotes Gastric Cancer Progression Through Regulating FOXF1/Wnt5a/beta-Catenin and MYOD1/Caspase-3 Signaling Pathways. *EBioMedicine* 2017;16:87–100. 10.1016/j.ebiom.2017.01.021. [PubMed: 28131747]
- [51]. Russell JC, Blue ME, Johnston MV, Naidu S, Hossain MA. Enhanced cell death in MeCP2 null cerebellar granule neurons exposed to excitotoxicity and hypoxia. *Neuroscience* 2007;150(3):563–74. 10.1016/j.neuroscience.2007.09.076. [PubMed: 17997046]
- [52]. Park H, Poo MM. Neurotrophin regulation of neural circuit development and function. *Nat Rev Neurosci* 2013;14(1):7–23. 10.1038/nrn3379. [PubMed: 23254191]
- [53]. Bramham CR, Messaoudi E. BDNF function in adult synaptic plasticity: the synaptic consolidation hypothesis. *Prog Neurobiol* 2005;76(2):99–125. 10.1016/j.pneurobio.2005.06.003. [PubMed: 16099088]
- [54]. Heldt SA, Stanek L, Chhatwal JP, Ressler KJ. Hippocampus-specific deletion of BDNF in adult mice impairs spatial memory and extinction of aversive memories. *Mol Psychiatry* 2007;12(7):656–70. 10.1038/sj.mp.4001957. [PubMed: 17264839]
- [55]. Notaras M, van den Buuse M. Neurobiology of BDNF in fear memory, sensitivity to stress, and stress-related disorders. *Mol Psychiatry* 2020;25(10):2251–74. 10.1038/s41380-019-0639-2. [PubMed: 31900428]
- [56]. Cao L, Jiao X, Zuzga DS, Liu Y, Fong DM, Young D, et al. VEGF links hippocampal activity with neurogenesis, learning and memory. *Nat Genet* 2004;36(8):827–35. 10.1038/ng1395. [PubMed: 15258583]
- [57]. Religa P, Cao R, Religa D, Xue Y, Bogdanovic N, Westaway D, et al. VEGF significantly restores impaired memory behavior in Alzheimer's mice by improvement of vascular survival. *Sci Rep* 2013;3:2053. 10.1038/srep02053. [PubMed: 23792494]
- [58]. Gondard E, Chau HN, Mann A, Tierney TS, Hamani C, Kalia SK, et al. . Rapid Modulation of Protein Expression in the Rat Hippocampus Following Deep Brain Stimulation of the Fornix. *Brain Stimul* 2015;8(6):1058–64. 10.1016/j.brs.2015.07.044. [PubMed: 26321354]
- [59]. Do-Monte FH, Rodriguez-Romaguera J, Rosas-Vidal LE, Quirk GJ. Deep brain stimulation of the ventral striatum increases BDNF in the fear extinction circuit. *Front Behav Neurosci* 2013;7:102. 10.3389/fnbeh.2013.00102. [PubMed: 23964215]
- [60]. Spieles-Engemann AL, Steece-Collier K, Behbehani MM, Collier TJ, Wohlgenant SL, Kemp CJ, et al. . Subthalamic nucleus stimulation increases brain derived neurotrophic factor in the nigrostriatal system and primary motor cortex. *J Parkinsons Dis* 2011;1(1):123–36. 10.3233/JPD-2011-11008. [PubMed: 22328911]
- [61]. Im HI, Hollander JA, Bali P, Kenny PJ. MeCP2 controls BDNF expression and cocaine intake through homeostatic interactions with microRNA-212. *Nat Neurosci* 2010;13(9):1120–7. 10.1038/nn.2615. [PubMed: 20711185]
- [62]. Li X, Liu X, Guo H, Zhao Z, Li YS, Chen G. The significance of the increased expression of phosphorylated MeCP2 in the membranes from patients with proliferative diabetic retinopathy. *Sci Rep* 2016;6:32850. 10.1038/srep32850. [PubMed: 27616658]
- [63]. Gallino D, Devenyi GA, Germann J, Guma E, Anastassiadis C, Chakravarty MM. Longitudinal assessment of the neuroanatomical consequences of deep brain stimulation: Application of fornical DBS in an Alzheimer's mouse model. *Brain Res* 2019;1715:213–23. 10.1016/j.brainres.2019.03.030. [PubMed: 30926457]
- [64]. Heschem S, Lim LW, Jahanshahi A, Steinbusch HW, Prickaerts J, Blokland A, et al. . Deep brain stimulation of the fornical area enhances memory functions in experimental dementia: the role of stimulation parameters. *Brain Stimul* 2013;6(1):72–7. 10.1016/j.brs.2012.01.008. [PubMed: 22405739]

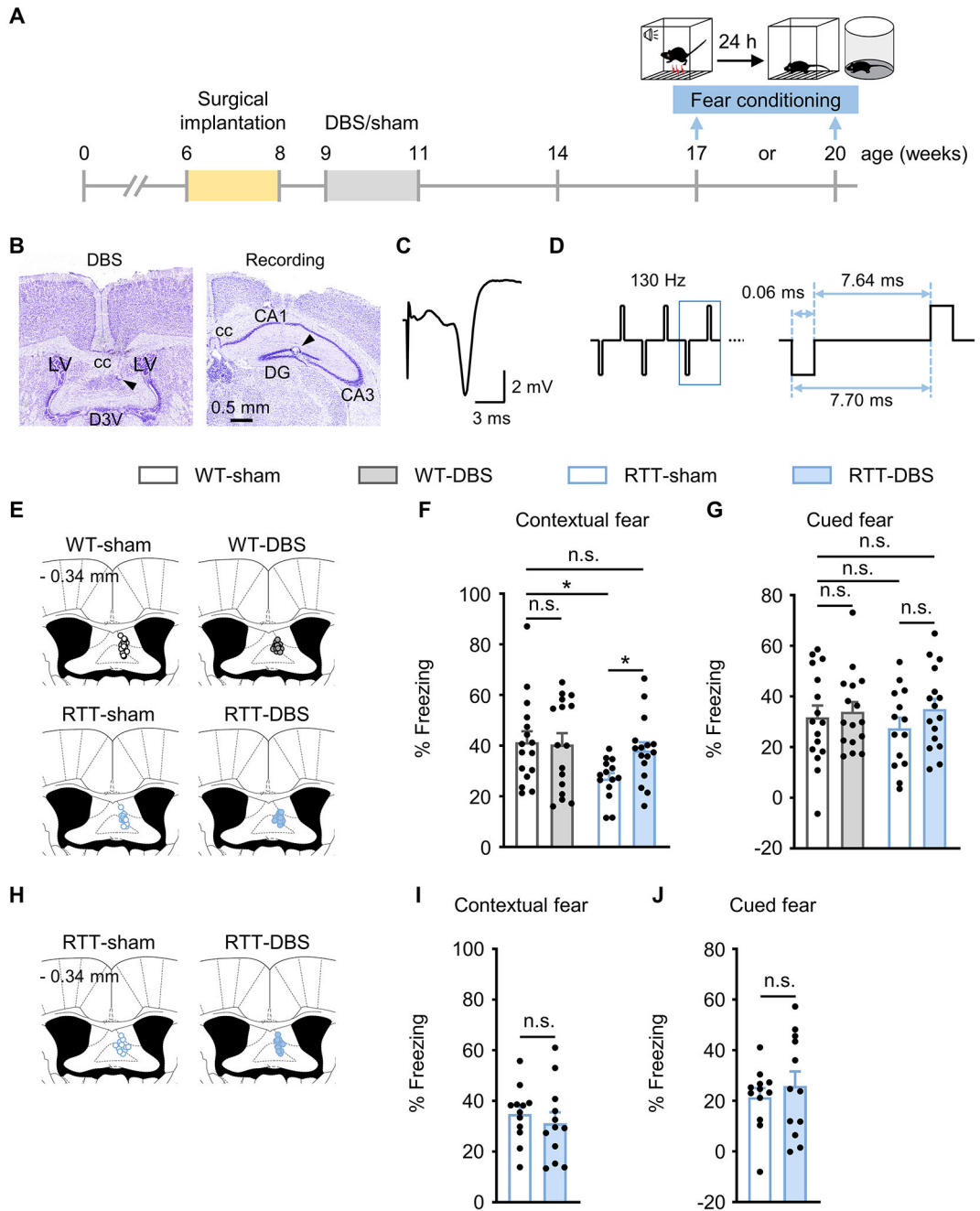
- [65]. Hescham S, Temel Y, Schipper S, Lagiery M, Schonfeld LM, Blokland A, et al. . Fornix deep brain stimulation induced long-term spatial memory independent of hippocampal neurogenesis. *Brain Struct Funct* 2017;222(2):1069–75. 10.1007/s00429-016-1188-y. [PubMed: 26832921]
- [66]. Li R, Zhang C, Rao Y, Yuan TF. Deep brain stimulation of fornix for memory improvement in Alzheimer’s disease: A critical review. *Ageing Res Rev* 2022;79:101668. 10.1016/j.arr.2022.101668. [PubMed: 35705176]
- [67]. Liu H, Temel Y, Boonstra J, Hescham S. The effect of fornix deep brain stimulation in brain diseases. *Cell Mol Life Sci* 2020;77(17):3279–91. 10.1007/s00018-020-03456-4. [PubMed: 31974655]
- [68]. Ranck JB Jr. Which elements are excited in electrical stimulation of mammalian central nervous system: a review. *Brain Res* 1975;98(3):417–40. 10.1016/0006-8993(75)90364-9. [PubMed: 1102064]
- [69]. Lozano AM, Lipsman N. Probing and regulating dysfunctional circuits using deep brain stimulation. *Neuron* 2013;77(3):406–24. 10.1016/j.neuron.2013.01.020. [PubMed: 23395370]
- [70]. Anderson RW, Farokhniaee A, Gunalan K, Howell B, McIntyre CC. Action potential initiation, propagation, and cortical invasion in the hyperdirect pathway during subthalamic deep brain stimulation. *Brain Stimul* 2018;11(5):1140–50. 10.1016/j.brs.2018.05.008. [PubMed: 29779963]
- [71]. BeMent SL, Ranck JB Jr. A quantitative study of electrical stimulation of central myelinated fibers. *Exp Neurol* 1969;24(2):147–70. 10.1016/0014-4886(69)90012-0. [PubMed: 5784129]
- [72]. Hescham S, Jahanshahi A, Schweimer JV, Mitchell SN, Carter G, Blokland A, et al. . Fornix deep brain stimulation enhances acetylcholine levels in the hippocampus. *Brain Struct Funct* 2016;221(8):4281–6. 10.1007/s00429-015-1144-2. [PubMed: 26597361]
- [73]. Ross EK, Kim JP, Settell ML, Han SR, Blaha CD, Min HK, et al. . Fornix deep brain stimulation circuit effect is dependent on major excitatory transmission via the nucleus accumbens. *Neuroimage* 2016;128:138–48. 10.1016/j.neuroimage.2015.12.056. [PubMed: 26780572]
- [74]. Fontaine D, Deudon A, Lemaire JJ, Razzouk M, Viau P, Darcourt J, et al. . Symptomatic treatment of memory decline in Alzheimer’s disease by deep brain stimulation: a feasibility study. *J Alzheimers Dis* 2013;34(1):315–23. 10.3233/JAD-121579. [PubMed: 23168448]
- [75]. Smith GS, Laxton AW, Tang-Wai DF, McAndrews MP, Diaconescu AO, Workman CI, et al. . Increased cerebral metabolism after 1 year of deep brain stimulation in Alzheimer disease. *Arch Neurol* 2012;69(9):1141–8. 10.1001/archneurol.2012.590. [PubMed: 22566505]
- [76]. Wang X, Hu WH, Zhang K, Zhou JJ, Liu DF, Zhang MY, et al. . Acute Fornix Deep Brain Stimulation Improves Hippocampal Glucose Metabolism in Aged Mice. *Chin Med J (Engl)* 2018;131(5):594–9. 10.4103/0366-6999.226067. [PubMed: 29483395]
- [77]. Stone SS, Teixeira CM, Devito LM, Zaslavsky K, Josselyn SA, Lozano AM, et al. . Stimulation of entorhinal cortex promotes adult neurogenesis and facilitates spatial memory. *J Neurosci* 2011;31(38):13469–84. 10.1523/JNEUROSCI.3100-11.2011. [PubMed: 21940440]
- [78]. Toda H, Hamani C, Fawcett AP, Hutchison WD, Lozano AM. The regulation of adult rodent hippocampal neurogenesis by deep brain stimulation. *J Neurosurg* 2008;108(1):132–8. 10.3171/JNS/2008/108/01/0132. [PubMed: 18173322]
- [79]. Liu A, Jain N, Vyas A, Lim LW. Ventromedial prefrontal cortex stimulation enhances memory and hippocampal neurogenesis in the middle-aged rats. *Elife* 2015;4. 10.7554/eLife.04803.
- [80]. Sorrells SF, Paredes MF, Cebrian-Silla A, Sandoval K, Qi D, Kelley KW, et al. . Human hippocampal neurogenesis drops sharply in children to undetectable levels in adults. *Nature* 2018;555(7696):377–81. 10.1038/nature25975. [PubMed: 29513649]
- [81]. Duque A, Arellano JI, Rakic P. An assessment of the existence of adult neurogenesis in humans and value of its rodent models for neuropsychiatric diseases. *Mol Psychiatry* 2022;27(1):377–82. 10.1038/s41380-021-01314-8. [PubMed: 34667259]
- [82]. Kempermann G, Gage FH, Aigner L, Song H, Curtis MA, Thuret S, et al. . Human Adult Neurogenesis: Evidence and Remaining Questions. *Cell Stem Cell* 2018;23(1):25–30. 10.1016/j.stem.2018.04.004. [PubMed: 29681514]
- [83]. Moreno-Jimenez EP, Terreros-Roncal J, Flor-Garcia M, Rabano A, Llorens-Martin M. Evidences for Adult Hippocampal Neurogenesis in Humans. *J Neurosci* 2021;41(12):2541–53. 10.1523/JNEUROSCI.0675-20.2020. [PubMed: 33762406]

- [84]. Kandel P, Semerci F, Mishra R, Choi W, Bajic A, Baluya D, et al. . Oleic acid is an endogenous ligand of TLX/NR2E1 that triggers hippocampal neurogenesis. *Proc Natl Acad Sci U S A* 2022;119(13):e2023784119. 10.1073/pnas.2023784119.
- [85]. Manganas LN, Zhang X, Li Y, Hazel RD, Smith SD, Wagshul ME, et al. . Magnetic resonance spectroscopy identifies neural progenitor cells in the live human brain. *Science* 2007;318(5852):980–5. 10.1126/science.1147851. [PubMed: 17991865]
- [86]. Temperli P, Ghika J, Villemure JG, Burkhard PR, Bogousslavsky J, Vingerhoets FJ. How do parkinsonian signs return after discontinuation of subthalamic DBS? *Neurology* 2003;60(1):78–81. 10.1212/wnl.60.1.78. [PubMed: 12525722]
- [87]. Vitek JL, Hashimoto T, Peoples J, DeLong MR, Bakay RA. Acute stimulation in the external segment of the globus pallidus improves parkinsonian motor signs. *Movement disorders : official journal of the Movement Disorder Society* 2004;19(8):907–15. 10.1002/mds.20137. [PubMed: 15300655]
- [88]. Benazzouz A, Hallett M. Mechanism of action of deep brain stimulation. *Neurology* 2000;55(12 Suppl 6):S13–6.
- [89]. Dostrovsky JO, Levy R, Wu JP, Hutchison WD, Tasker RR, Lozano AM. Microstimulation-induced inhibition of neuronal firing in human globus pallidus. *Journal of neurophysiology* 2000;84(1):570–4. 10.1152/jn.2000.84.1.570. [PubMed: 10899228]
- [90]. Lowet E, Kondabolu K, Zhou S, Mount RA, Wang Y, Ravasio CR, et al. . Deep brain stimulation creates informational lesion through membrane depolarization in mouse hippocampus. *Nat Commun* 2022;13(1):7709. 10.1038/s41467-022-35314-1. [PubMed: 36513664]
- [91]. Xia F, Yiu A, Stone SSD, Oh S, Lozano AM, Josselyn SA, et al. . Entorhinal Cortical Deep Brain Stimulation Rescues Memory Deficits in Both Young and Old Mice Genetically Engineered to Model Alzheimer’s Disease. *Neuropsychopharmacology* 2017;42(13):2493–503. 10.1038/npp.2017.100. [PubMed: 28540926]
- [92]. Whittle N, Schmuckermair C, Gunduz Cinar O, Hauschild M, Ferraguti F, Holmes A, et al. . Deep brain stimulation, histone deacetylase inhibitors and glutamatergic drugs rescue resistance to fear extinction in a genetic mouse model. *Neuropharmacology* 2013;64:414–23. 10.1016/j.neuropharm.2012.06.001. [PubMed: 22722028]
- [93]. Charvet CJ, Finlay BL. Comparing Adult Hippocampal Neurogenesis Across Species: Translating Time to Predict the Tempo in Humans. *Front Neurosci* 2018;12:706. 10.3389/fnins.2018.00706. [PubMed: 30344473]
- [94]. Miranda M, Morici JF, Zanoni MB, Bekinschtein P. Brain-Derived Neurotrophic Factor: A Key Molecule for Memory in the Healthy and the Pathological Brain. *Front Cell Neurosci* 2019;13:363. 10.3389/fncel.2019.00363. [PubMed: 31440144]
- [95]. Kowianski P, Lietzau G, Czuba E, Waskow M, Steliga A, Morys J. BDNF: A Key Factor with Multipotent Impact on Brain Signaling and Synaptic Plasticity. *Cell Mol Neurobiol* 2018;38(3):579–93. 10.1007/s10571-017-0510-4. [PubMed: 28623429]
- [96]. Jeanneteau F, Arango-Lievano M, Chao MV. Synapse Development and Maturation (second edition). Chapter 7-Neurotrophin and synaptogenesis. Elsevier Inc. 2020:167–92.
- [97]. Faust K, Vajkoczy P, Xi B, Harnack D. The Effects of Deep Brain Stimulation of the Subthalamic Nucleus on Vascular Endothelial Growth Factor, Brain-Derived Neurotrophic Factor, and Glial Cell Line-Derived Neurotrophic Factor in a Rat Model of Parkinson’s Disease. *Stereotact Funct Neurosurg* 2021;99(3):256–66. 10.1159/000511121. [PubMed: 33152730]
- [98]. Chang Q, Khare G, Dani V, Nelson S, Jaenisch R. The disease progression of Mecp2 mutant mice is affected by the level of BDNF expression. *Neuron* 2006;49(3):341–8. 10.1016/j.neuron.2005.12.027. [PubMed: 16446138]
- [99]. Ehinger Y, Bruyere J, Panayotis N, Abada YS, Borloz E, Matagne V, et al. . Huntingtin phosphorylation governs BDNF homeostasis and improves the phenotype of Mecp2 knockout mice. *EMBO Mol Med* 2020;12(2):e10889. 10.15252/emmm.201910889. [PubMed: 31913581]
- [100]. Kernie SG, Liebl DJ, Parada LF. BDNF regulates eating behavior and locomotor activity in mice. *EMBO J* 2000;19(6):1290–300. 10.1093/emboj/19.6.1290. [PubMed: 10716929]

- [101]. Takahashi Y, Enatsu R, Kanno A, Imataka S, Komura S, Tamada T, et al. . Comparison of Thresholds between Bipolar and Monopolar Electrical Cortical Stimulation. *Neurol Med Chir (Tokyo)* 2022;62(6):294–9. 10.2176/jns-nmc.2021-0389. [PubMed: 35466117]
- [102]. Shirvalkar PR, Rapp PR, Shapiro ML. Bidirectional changes to hippocampal theta-gamma comodulation predict memory for recent spatial episodes. *Proc Natl Acad Sci U S A* 2010;107(15):7054–9. 10.1073/pnas.0911184107. [PubMed: 20351262]
- [103]. Mohan UR, Watrous AJ, Miller JF, Lega BC, Sperling MR, Worrell GA, et al. . The effects of direct brain stimulation in humans depend on frequency, amplitude, and white-matter proximity. *Brain Stimul* 2020;13(5):1183–95. 10.1016/j.brs.2020.05.009. [PubMed: 32446925]
- [104]. Kang E, Wen Z, Song H, Christian KM, Ming GL. Adult Neurogenesis and Psychiatric Disorders. *Cold Spring Harb Perspect Biol* 2016;8(9). 10.1101/cshperspect.a019026.
- [105]. Kim IB, Park SC. The Entorhinal Cortex and Adult Neurogenesis in Major Depression. *Int J Mol Sci* 2021;22(21). 10.3390/ijms222111725.

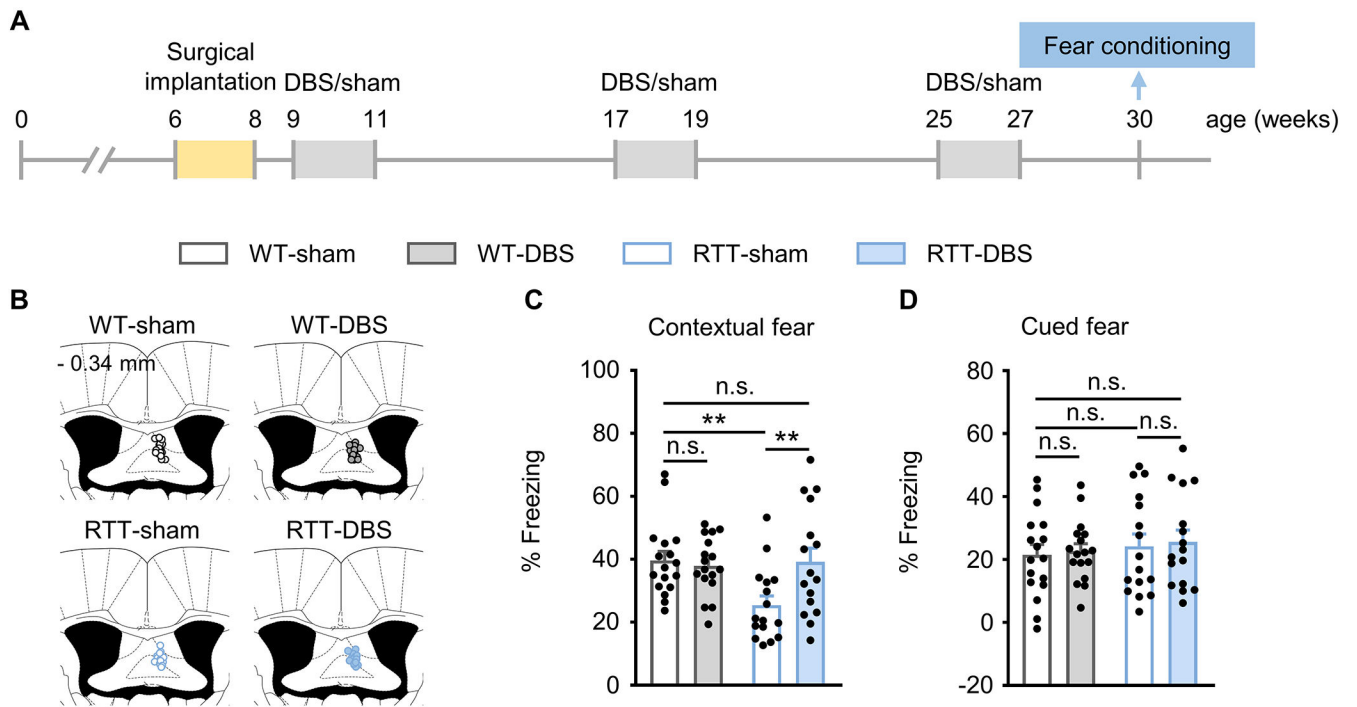
HIGHLIGHTS

- Memory enhancement persists weeks after forniceal DBS treatment
- Repeated DBS treatment maintains memory benefit
- DBS skews neurogenesis toward MeCP2-positive cells
- DBS stimulates BDNF expression in the hippocampus

**Fig. 1.**

Forniceal DBS-induced fear memory benefit lasts at least 6 weeks but not 9 weeks. (A) Experimental timeline. Female RTT and WT mice were implanted with DBS electrodes at 6 - 8 weeks of age and received daily DBS/sham treatment for 2 weeks. To test fear memory, separate cohorts of mice experienced fear conditioning task 6 and 9 weeks after DBS/sham treatment, respectively. (B) Photomicrographs illustrating DBS electrode placement (arrowhead) in the fimbria-fornix (*left*) and the recording electrode in the dentate gyrus (*right*). cc, corpus callosum; LV, lateral ventricle; D3V, dorsal third ventricle; DG, dentate

gyrus. (C) Representative evoked potential trace of the fimbria-fornix pathway recorded in the dentate gyrus. (D) Schematic of the DBS pulse pattern and parameters. (E-G) Fear memory 6 weeks after DBS. (E) Schematic representation of the fimbria-fornix for the targeting sites of DBS electrodes. The number on the top left represents the posterior coordinate from the bregma. Contextual (F) and cued (G) freezing responses 6 weeks after DBS/sham in RTT and WT mice (17-week-old; WT-sham, $n = 16$; WT-DBS, $n = 16$; RTT-sham, $n = 14$; RTT-DBS, $n = 16$). Two-way ANOVA followed by Tukey *post hoc*. Contextual: genotype, $F_{1,58} = 4.921$, $p = 0.030$; treatment, $F_{1,58} = 1.807$, $p = 0.184$. Cued: genotype, $F_{1,58} = 0.144$, $p = 0.706$; treatment, $F_{1,58} = 1.360$, $p = 0.248$. (H-J) Fear memory 9 weeks after DBS. (H) Schematic representation of the fimbria-fornix for the targeting sites of DBS electrodes. The number on the top left represents the posterior coordinate from the bregma. Contextual (I) and cued (J) freezing responses 9 weeks after DBS/sham in RTT mice (20-week-old; $n = 12$ mice per group). Contextual: two-tailed unpaired *t*-test, $p = 0.504$. Cued: Mann-Whitney test, $p = 0.751$. * $p < 0.05$; n.s., not significant. Data presented as mean \pm SEM with individual values.

**Fig. 2.**

Repeated forniceal DBS maintains the memory benefit. (A) Experimental timeline. One week after DBS electrode implantation, mice received 3 sessions of 2-week DBS/sham treatment separated by 6 weeks. Fear memory was evaluated 3 weeks after the last day of DBS/sham treatment in all groups of mice (30-week-old). (B) Schematic representation of the fimbria-fornix for the targeting sites of DBS electrodes. The numbers on the top left represent the posterior coordinate from the bregma. (C, D) Contextual (C) and cued (D) freezing responses in RTT mice and WT controls (WT-sham, $n = 17$; WT-DBS, $n = 17$; RTT-sham, $n = 16$; RTT-DBS, $n = 16$). Two-way ANOVA followed by Tukey *post hoc*. Contextual: genotype, $F_{1,62} = 4.152$, $p = 0.046$; treatment, $F_{1,62} = 3.633$, $p = 0.061$. Cued: genotype, $F_{1,62} = 0.687$, $p = 0.410$; treatment, $F_{1,62} = 0.142$, $p = 0.707$. ** $p < 0.01$; n.s., not significant. Data presented as mean \pm SEM with individual values.

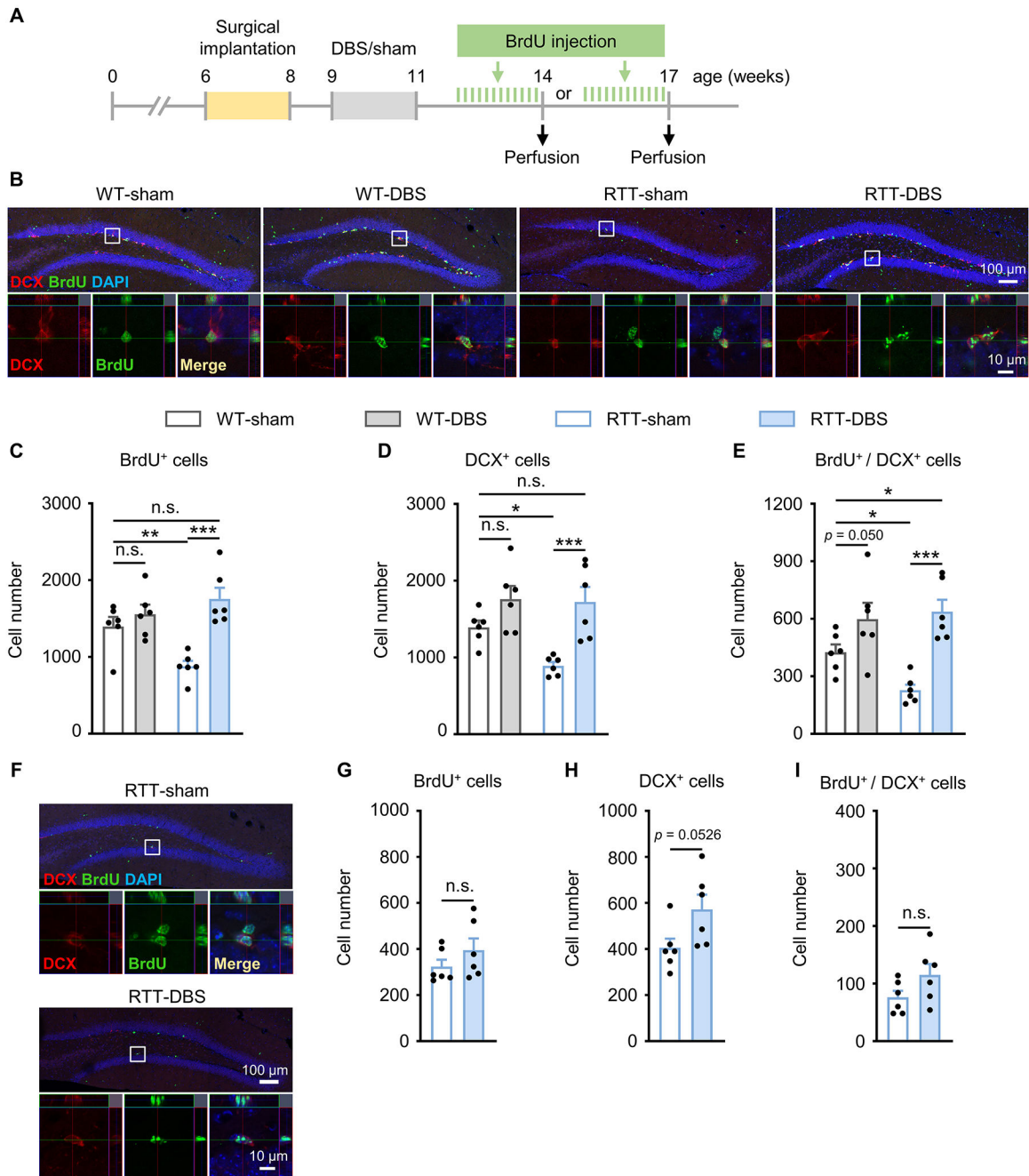
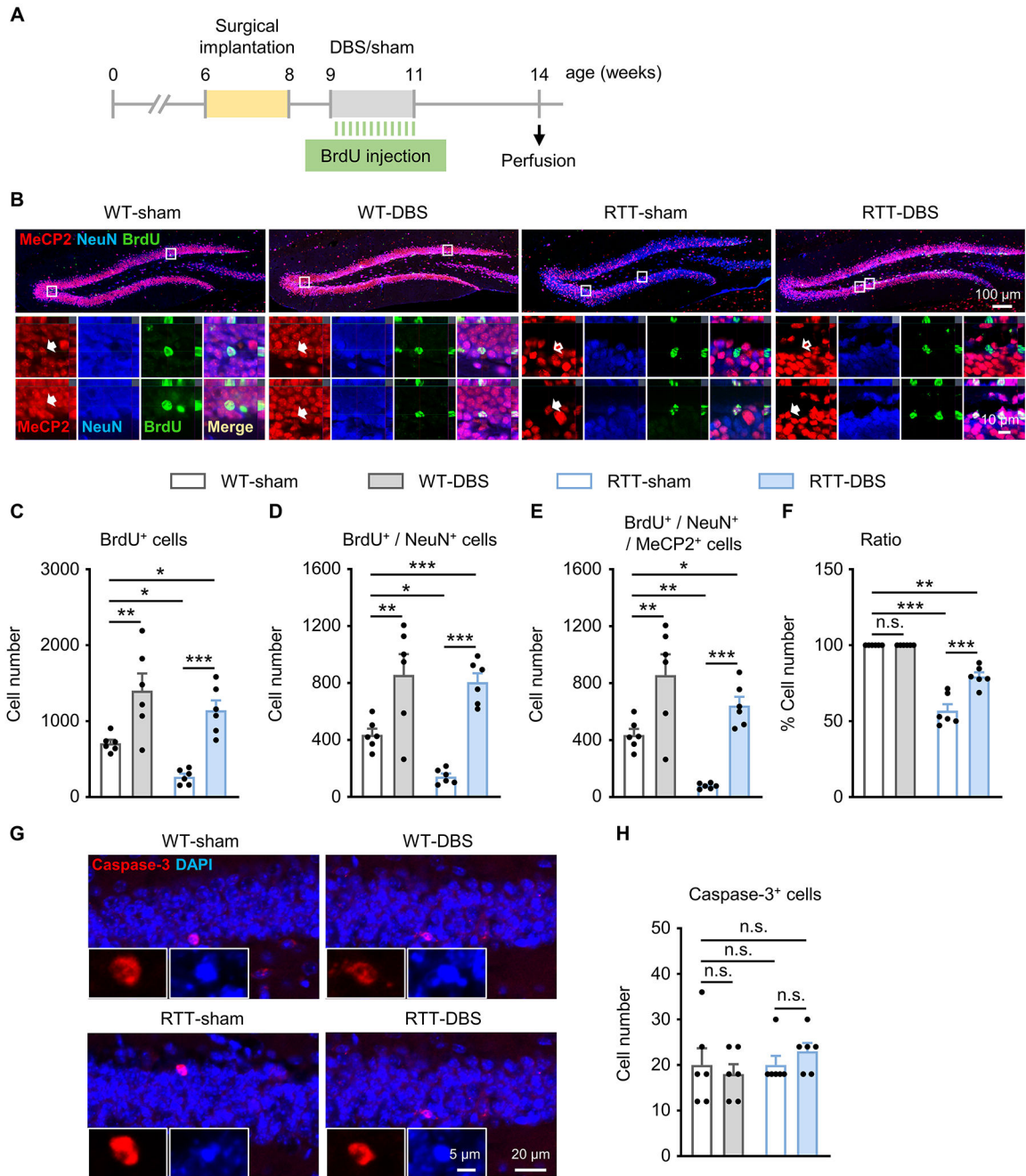


Fig. 3. Increased hippocampal neurogenesis induced by forniceal DBS lasts for at least 3 weeks but not as long as 6 weeks. (A) Experimental timeline. RTT mice and WT littermates were implanted with DBS electrodes at 6 - 8 weeks of age and received daily DBS/sham treatment for 2 weeks after surgery. To evaluate neurogenesis in the dentate gyrus 3 and 6 weeks after DBS/sham, two separate cohorts of mice were treated with BrdU (75 mg/kg, i.p.) for 12 days before perfusion, respectively. (B, C, D, E) Neurogenesis 3 weeks after DBS/sham in RTT mice and WT littermates (14-week-old, n = 6 mice per group). Representative

images at low (*top*) and high (*bottom*) magnification showing DCX⁺ cells (red), BrdU⁺ cells (green), DAPI (blue), and the merge (yellow) from each of the four groups (B). Newborn neurons are located in the innermost layer of the dentate gyrus. Two-way ANOVA followed by Tukey *post hoc* revealed a significant treatment main effect on the numbers of BrdU⁺ cells (C, $F_{1,20} = 18.908$, $p < 0.001$), DCX⁺ cells (D, $F_{1,20} = 18.643$, $p < 0.001$), and BrdU⁺ / DCX⁺ double staining cells (E, $F_{1,20} = 24.659$, $p < 0.001$). (F, G, H, I) Neurogenesis 6 weeks after DBS/sham treatment in RTT mice (17-week-old, n = 6 mice per group). Representative images at low (*top*) and high (*bottom*) magnification showing DCX⁺ cells (red), BrdU⁺ cells (green), DAPI (blue), and the merge (yellow) from RTT-sham and RTT-DBS groups (F). The two-tailed unpaired *t*-test revealed no difference in the number of BrdU⁺ cells (G, $p = 0.258$), DCX⁺ cells (H, $p = 0.0526$), and BrdU⁺ / DCX⁺ double staining cells (I, $p = 0.113$) between RTT-DBS and RTT-sham mice. * $p < 0.05$, ** $p < 0.01$, *** $p < 0.001$. n.s., not significant. Data presented as mean \pm SEM with individual values.

**Fig. 4.**

Forniceal DBS induces birth of more MeCP2⁺ than MeCP2⁻DGCs without affecting neuronal survival in RTT mice. (A) Experimental timeline. (B) Representative images at low (*top*) and high (*bottom*) magnification showing MeCP2⁺ cells (red), NeuN⁺ cells (blue), BrdU⁺ cells (green), and the merge (yellow) from each of the four groups. Filled arrow, MeCP2⁺ cells; empty arrow, MeCP2⁻ cells. (C, D, E, F) Summary of immunoreactive cell counting ($n = 6$ mice per group). Two-way ANOVA followed by Tukey *post hoc* revealed a significant main effect on the numbers of BrdU⁺ cells (C, genotype, $F_{1,20} = 6.680$, $p =$

0.018; treatment, $F_{1,20} = 33.761$, $p < 0.001$), BrdU⁺ / NeuN⁺ cells (D, genotype, $F_{1,20} = 4.263$, $p = 0.052$; treatment, $F_{1,20} = 42.171$, $p < 0.001$), BrdU⁺ / NeuN⁺ / MeCP2⁺ cells (E, genotype, $F_{1,20} = 11.999$, $p = 0.002$; treatment, $F_{1,20} = 35.509$, $p < 0.001$), and the ratio of BrdU⁺ / NeuN⁺ / MeCP2⁺ cells over total BrdU⁺ / NeuN⁺ cells (F, genotype, $F_{1,20} = 160.717$, $p < 0.001$; treatment, $F_{1,20} = 20.208$, $p < 0.001$). (G) Representative images stained with caspase-3 (red) and DAPI (blue) in the dentate gyrus. Inset, caspase-3 positive cells at higher magnification. (H) Number of caspase-3 positive cells in each of the 4 study groups (n = 6 mice per group). Two-way ANOVA followed by Tukey *post hoc*: genotype, $F_{1,20} = 0.969$, $p = 0.337$; treatment, $F_{1,20} = 0.039$, $p = 0.846$. * $p < 0.05$, ** $p < 0.01$, *** $p < 0.001$. n.s., not significant. Data presented as mean \pm SEM with individual values.

Author Manuscript

Author Manuscript

Author Manuscript

Author Manuscript

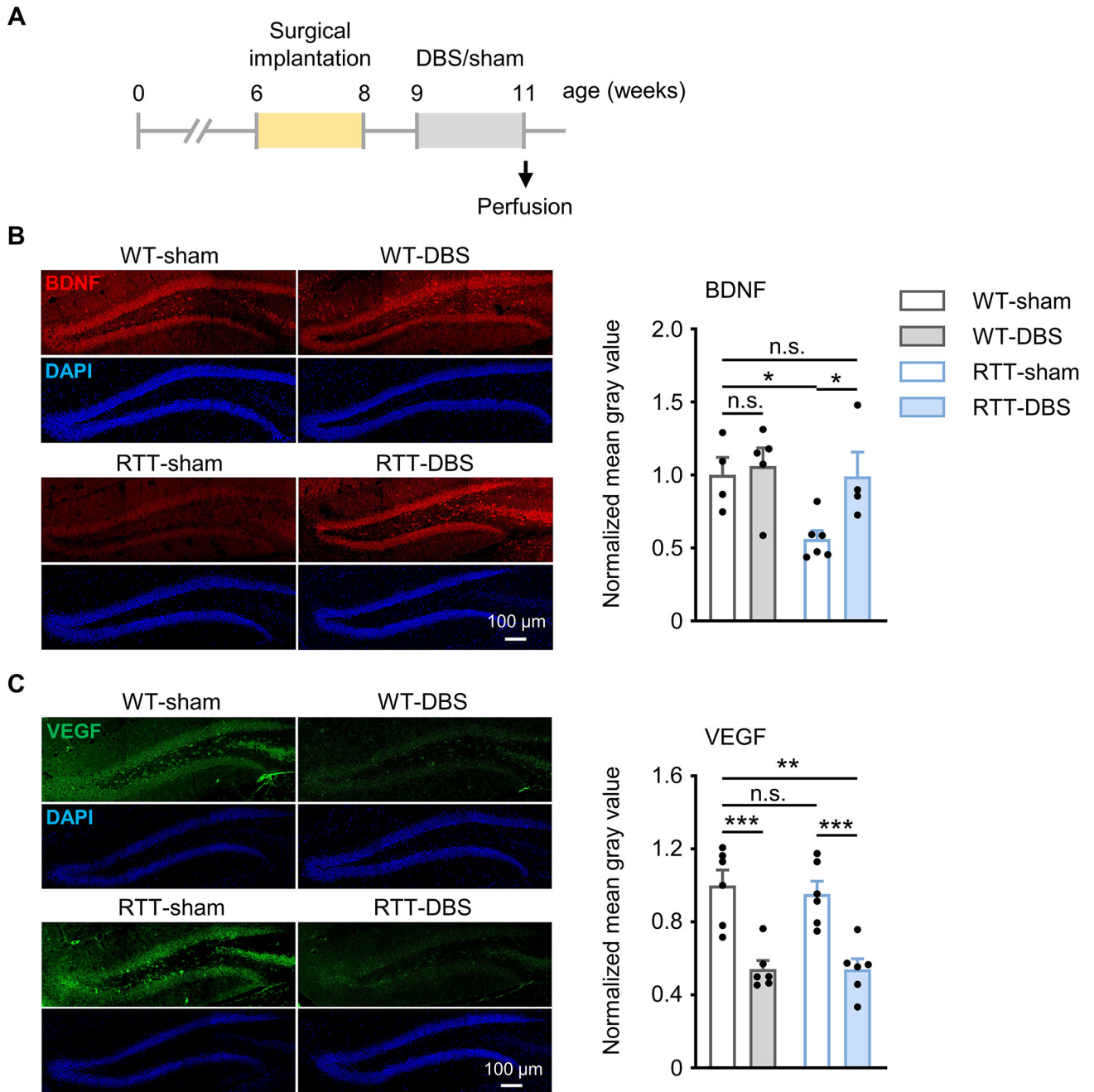


Fig. 5. Forniceal DBS increases BDNF expression in RTT mice and decreases VEGF expression in both WT and RTT mice. (A) Experimental timeline. (B) (*left*) Representative images stained with BDNF (red) and DAPI (blue) in the dentate gyrus; (*right*) Quantification of BDNF expression in the 4 study groups (WT-sham, $n = 4$; WT-DBS, $n = 5$; RTT-sham, $n = 6$; RTT-DBS, $n = 4$). Two-way ANOVA followed by Tukey *post hoc*: genotype, $F_{1,15} = 4.875$, $p = 0.043$; treatment, $F_{1,15} = 4.507$, $p = 0.051$. (C) (*left*) Representative images stained with VEGF (green) and DAPI (blue) in the dentate gyrus; (*right*) Quantification of

VEGF expression in the 4 study groups (n = 6 mice per group). Two-way ANOVA followed by Tukey *post hoc*: genotype, $F_{1,20} = 0.132$, $p = 0.720$; treatment, $F_{1,20} = 43.043$, $p < 0.001$. * $p < 0.05$, ** $p < 0.01$, *** $p < 0.001$. n.s., not significant. Data presented as mean \pm SEM with individual values.

Author Manuscript

Author Manuscript

Author Manuscript

Author Manuscript